the FEBS Journal

Role of phosphate in the central metabolism of two lactic acid bacteria – a comparative systems biology approach

Jennifer Levering[1,*], Mark W. J. M. Musters[2,3,*], Martijn Bekker[4,*], Domenico Bellomo[3,5], Tomas Fiedler[6], Willem M. de Vos[2], Jeroen Hugenholtz[3,4], Bernd Kreikemeyer[6], Ursula Kummer[1] and Bas Teusink[3,5]

1 Department of Modeling of Biological Processes, COS Heidelberg/BIOQUANT, University of Heidelberg, Germany
2 Laboratory of Microbiology, Wageningen University, The Netherlands
3 Kluyver Centre for Genomics of Industrial Fermentation, Delft, The Netherlands
4 Laboratory for Microbiology, Swammerdam Institute for Life Sciences, Amsterdam, The Netherlands
5 Systems Bioinformatics IBIVU/Netherlands Consortium for Systems Biology, Faculty of Earth and Life Sciences, Vrije Universiteit Amsterdam, The Netherlands
6 Institute of Medical Microbiology, Virology and Hygiene, Rostock, Germany

Keywords
glycolysis; kinetic modelling; *Lactococcus lactis*; phosphate uptake; *Streptococcus pyogenes*

Correspondence
B. Teusink, Systems Bioinformatics IBIVU/Netherlands Consortium for Systems Biology, Faculty of Earth and Life Sciences, Vrije Universiteit Amsterdam, De Boelelaan 1085, 1081 HV Amsterdam, The Netherlands
Fax: +31(0)205989435
Tel: + 31(0)205989435
E-mail: b.teusink@vu.nl

*These authors contributed equally to this work.

(Received 14 June 2011, revised 24 January 2012, accepted 3 February 2012)

doi:10.1111/j.1742-4658.2012.08523.x

Lactic acid-producing bacteria survive in distinct environments, but show common metabolic characteristics. Here we studied the dynamic interactions of the central metabolism in *Lactococcus lactis*, extensively used as a starter culture in the dairy industry, and *Streptococcus pyogenes*, a human pathogen. Glucose-pulse experiments and enzymatic measurements were performed to parameterize kinetic models of glycolysis. Significant improvements were made to existing kinetic models for *L. lactis*, which subsequently accelerated the development of the first kinetic model of *S. pyogenes* glycolysis. The models revealed an important role for extracellular phosphate in the regulation of central metabolism and the efficient use of glucose. Thus, phosphate, which is rarely taken into account as an independent species in models of central metabolism, should be considered more thoroughly in the analysis of metabolic systems in the future. Insufficient phosphate supply can lead to a strong inhibition of glycolysis at high glucose concentrations in both species, but this was more severe in *S. pyogenes*. *S. pyogenes* is more efficient at converting glucose to ATP, showing a higher tendency towards heterofermentative energy metabolism than *L. lactis*. Our comparative systems biology approach revealed that the glycolysis of *L. lactis* and *S. pyogenes* have similar characteristics, but are adapted to their individual natural habitats with respect to phosphate regulation.

Database
The mathematical models described here have been submitted to the Online Cellular Systems Modelling Database and can be accessed at http://jjj.biochem.sun.ac.za/database/Levering/index.html free of charge.

Abbreviations
2-PGA, 2-phosphoglycerate; 3-PGA, 3-phosphoglycerate; Fru(1,6)P_2, fructose 1,6-bisphosphate; GA3P, glyceraldehyde 3-phosphate; GAPDH, glyceraldehyde-3-phosphate dehydrogenase; GAPN, non-phosphorylating $NADP^+$-dependent glyceraldehyde-3-phosphate dehydrogenase; Glc6*P*, glucose 6-phosphate; HPr, a low-molecular-weight, heat-stable protein, part of PTS; HPr-ser-P, serine-phosphorylated HPr; LDH, L-lactate dehydrogenase; NTP, nucleoside triphosphate; PaseII, HPr(ser-P)-activated sugar-phosphate phosphatase II; P_i, unbound inorganic phosphate; PTS, phosphotransferase system; triose-P, GA3P and dihydroxyacetone.

Introduction

Lactic acid-producing bacteria are Gram-positive bacteria that survive in distinct biotopes, including foods and plants, and even the human body [1]. Some lactic acid-producing bacteria play an essential role in the fermented food and beverage industry, while others possess pathogenic features. Therefore, the impact of this type of bacteria on our daily life is significant. There is great biodiversity amongst lactic acid-producing bacteria with respect to their genetics and consequent biochemistry alternatively metabolism would also be better, which is reflected in differences in flavour production, acidification rates, pathogenicity and health benefits. Such diversity has been studied using various comparative and pan-genomics focus on the full complement of genes of an organism [2–6]. In this paper we illustrate the use of a comparative systems biology approach. Comparative systems biology tries to understand similarities and differences in behaviour as a result of how the components interact dynamically. Moreover, similarly to the way that comparative genomics provides a knowledge base, comparative systems biology holds the promise of accelerating model development.

Here, our comparative systems biology approach focused on the primary metabolism of two specific lactic acid-producing bacteria: the beneficial *Lactococcus lactis*, frequently used in dairy products, and the human pathogen *Streptococcus pyogenes*. *L. lactis* is a nonpathogenic, noninvasive, noncolonizing and facultative anaerobic bacterium that can be found on plants and within the digestive tract of cows, but is mostly studied for its use in dairy fermentations [7]. *S. pyogenes* colonizes the skin or throat and causes many important human diseases, ranging from mild superficial infections of the skin and mucous membranes of the nasopharynx to severe systemic and invasive diseases [8]. Thus, the natural environments of *L. lactis* and *S. pyogenes* differ considerably in nutrients, temperature, oxygen availability and pH, but the similarities in their central metabolism are striking: they essentially ferment glucose to lactic acid and rely on substrate-level phosphorylation for ATP synthesis. In general, *S. pyogenes* and *L. lactis* are reported to be homofermentative and convert sugars primarily to generate energy [9]. Moreover, under certain conditions, such as glucose limitation, the metabolism of these bacteria shifts from homolactic to mixed-acid fermentation, resulting in the production of formate, acetate and ethanol [10,11].

In contrast to *L. lactis*, the dynamics of the *S. pyogenes* metabolism has barely been studied. Some *S. pyogenes*-specific allosteric regulations of glycolysis have been identified, but no dynamic model of *S. pyogenes* glycolysis exists to evaluate the impact of these. The focus has been particularly on the molecular mechanisms behind virulence rather than on metabolism. We used a comparative systems biology approach to accelerate the construction of a kinetic model for the poorly studied *S. pyogenes*, starting with a well-described model of *L. lactis* glycolysis and subsequent improvement by a limited set of model-driven measurements on enzyme kinetics and metabolic analyses upon glucose perturbations.

Several kinetic models have been developed for *L. lactis* glycolysis by us and others, to study metabolic flux distributions [12,13], metabolic regulation [14,15] and pH control [16]. Upon inspection, these models have limitations in their ability to fit phosphate-containing species, in particular the fructose-1,6-bisphosphate [Fru(1,6)P_2] levels [13,16]. In the current communication we present (a) an improved kinetic model of *L. lactis* glycolysis, which accurately simulates our measured metabolite profiles quantitatively and is also consistent with published ^{13}C- and ^{31}P-NMR data [17], (b) the first kinetic model of *S. pyogenes* glycolysis, constructed using the *L. lactis* model as a blueprint to accelerate model development (the model reproduces our measured metabolite profiles for this species) and (c) a comparison of the dynamics of glycolysis in both lactic acid-producing bacteria, with a special focus on the allosteric regulation by extracellular phosphate. The comparison revealed differences in *S. pyogenes* and *L. lactis* that are robust against parameter uncertainties and make sense in the light of differences in the phosphate levels of their natural environment.

Therefore, comparative systems biology comprises an experimental and modelling approach to efficiently study systems properties that are responsible for differences in the behaviour of distinct, yet closely related, organisms.

Results

Kinetic modelling of *L. lactis* uncovers imbalance in phosphate pools of NMR data

At the start of our study, we tested existing models for their ability to describe published data sets. We found that previous models consistently predict maximum Fru(1,6)P_2 levels of $\sim$ 20 mM [13,16], while measured Fru(1,6)P_2 levels reached values of 50 mM [17]. Upon inspection, we found a mismatch between the

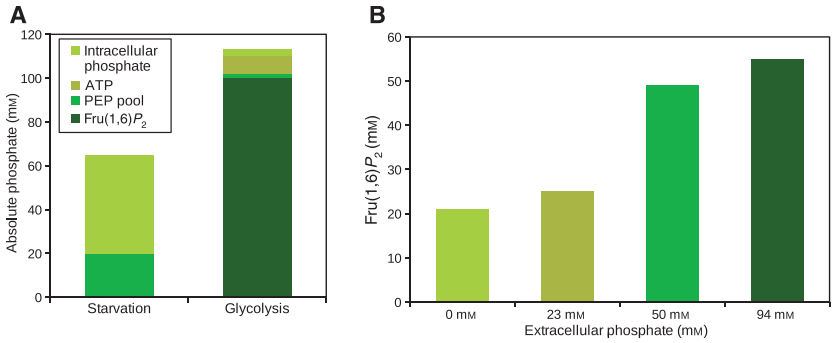

Fig. 1. Influence of extracellular phosphate on intracellular phosphate pools. (A) Differences in phosphate pools in the experiments of Neves *et al.* [17]. During starvation, the major phosphate pools are intracellular P_i and the phospho*enol*pyruvate pool [3-PGA, 2-PGA and phospho*enol*pyruvate (PEP)]. The total amount of phosphate in glycolytic intermediates is 65 mM. However, during glycolysis, most phosphate is incorporated in Fru(1,6)P_2. Fru(1,6)P_2 contains two moles of phosphate per mole of Fru(1,6)P_2, so 50 mM Fru(1,6)P_2 is equivalent to 100 mM phosphate. ATP contains three moles of phosphate, but contains net one mole of phosphate during glycolysis if all adenosine moieties are assumed to be constant during the experiment. The difference in phosphate content between starvation and glycolysis is about 50 mM. In addition, the short timescale ($\sim$ 1 min) at which 50 mM phosphate appears cannot be explained by depleting other phosphate resources, such as phosphate from phosphorylated glycolytic intermediates with inducer expulsion [71], polyphosphate [72] or pyrophosphate [19]. (B) Based on the literature, buffers with 0, 23, 50 and 94 mM [10,21–23] extracellular phosphate have a different effect on the Fru(1,6)P_2 levels of *Lactococcus lactis* during glycolysis.

total measured phosphate pool under starved and glycolysing conditions. Phosphate is primarily incorporated in the phospho*enol*pyruvate pool (3-PGA, 2-PGA and phosphoenolpyruvate) (about 20 mM) and as unbound inorganic phosphate (P_i) (45 mM) during starvation, and shifts towards Fru(1,6)P_2 (50 mM) and ATP (8 mM) during glycolysis. The sum of the total measured phosphate concentration is therefore $\sim$ 60 mM during starvation but $\sim$ 110 mM during glycolysis (Fig. 1A). Hereby, we assume that Fru(1,6)P_2 and ATP are almost depleted in starving cells because these are the levels to which the cells return after using up all glucose. Unidentified phosphorylated compounds [18–20] or phosphate in the cell wall are not likely to explain this difference of $\sim$ 50 mM between these two physiological states, as the disappearance of phosphate upon starvation shows such fast kinetics.

To quantify intracellular metabolites, Neves and coworkers performed ^{13}C-NMR experiments in 50 mM KP_i buffer [17]. However, they repeated their measurements of P_i and nucleoside triphosphates (NTPs) with ^{31}P-NMR in a phosphate-free Mes/KOH buffer, to allow measurements of P_i and NTPs. A subsequent literature survey showed that the concentration of phosphate in the medium appears to have a pronounced effect on the intracellular Fru(1,6)P_2 concentration during glucose consumption. Thus, it appears that the Fru(1,6)P_2 pools increase with the extracellular phosphate concentration [10,21–23] (see Fig. 1B). This implies that the pool of free and bound phosphate [in phospho*enol*pyruvate, Fru(1,6)P_2 and so forth] is critically dependent on the external phosphate concentration.

We carried out experiments similar to those performed by Neves *et al.* [17] by use of NAD^+/$NADP^+$-coupled enzymatic assays. This revealed a dependency of the build-up of Fru(1,6)P_2 on the extracellular phosphate concentration (see Fig. 2 and Fig. S1). Therefore, we concluded that the observed differences in the total phosphate pool between glycolysing and starving cells is probably a result of differences in external phosphate concentrations. In summary, we have shown that the internal phosphate pool depends on the extracellular phosphate concentrations, which implies that the phosphate exchange over the membrane should be included in the respective kinetic models.

Quantitative simulation of the dynamic profiles of glycolytic intermediates in *L. lactis*

Setting up the kinetic model for *L. lactis* on the basis of existing models necessitated a (re)assessment of all relevant processes and their respective regulation, as described later in this paragraph. In *L. lactis*, the main part of the external sugar is taken up via the high-affinity phospho*enol*pyruvate-dependent phosphotransferase system (PTS; EC 2.7.1.69) and is converted directly into glucose 6-phosphate (Glc6*P*) [24], which is modelled as a single-step reaction for *L. lactis*. A low-affinity glucose permease is present, but its contribution to the overall uptake of glucose is limited [25]. Therefore, we omitted this permease in our model. The conversion of

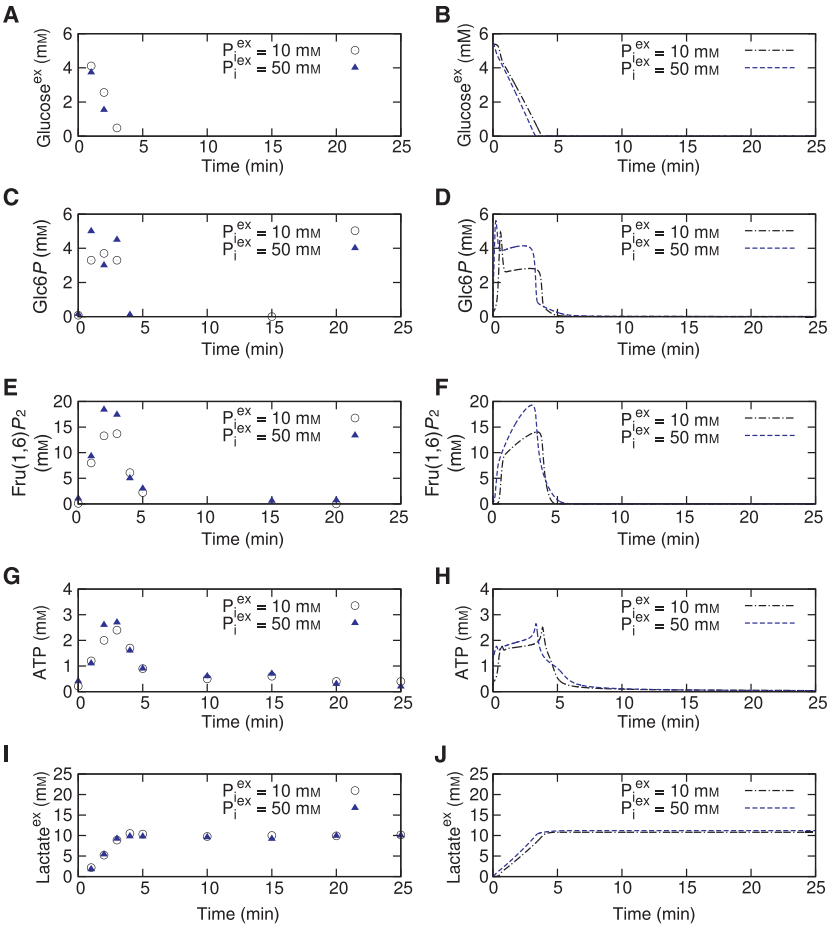

Fig. 2. Metabolic profiles and model simulations of 5 mM glucose-pulse experiments in *Lactococcus lactis*. We measured the effect of 10 mM (circles) and 50 mM (triangles) extracellular P_i on the profiles of (A) external glucose, (C) Glc6*P*, (E) Fru(1,6)P_2, (G) ATP and (I) extracellular lactate; (B), (D), (F), (H) and (J) show the corresponding model simulations. The simulations were performed with a measured intracellular to extracellular volume ratio (based on measurements of the absorbance at 600 nm) of 0.034417 and 0.029, respectively; the initial concentrations at 10 and 50 mM extracellular phosphate are given in Table S6.

glucose to its product pyruvate proceeds via the Embden–Meyerhof–Parnas pathway. Thereby, the pyruvate kinase (EC 2.7.1.40) is allosterically activated by Fru(1,6)P_2 and inhibited by P_i [26]. Under conditions of glucose excess, the majority of pyruvate synthesized is converted into lactate, a process catalysed by L-lactate dehydrogenase (LDH; EC 1.1.1.27). LDH in *L. lactis* is allosterically activated and inhibited by Fru(1,6)P_2 and P_i, respectively [27]. The pyruvate formate-lyase (EC 2.3.1.54) is inhibited by glyceraldehyde 3-phosphate (GA3P) [28,29]. Acetyl CoA is metabolized to acetate via acetylphosphate or, alternatively, via acetaldehyde to ethanol [10]. The compounds acetate, ethanol and formate are synthesized and subsequently transported out of the cell. An ATPase reaction is included as a sink for the ATP generated in glycolysis, replacing all ATP-consuming reactions.

To account for the influence of external phosphate concentrations on the metabolic intermediates during glycolysis, we included phosphate exchange over the cytoplasmic membrane. Therefore, we extended the model with an ATP-driven phosphate uniporter in *L. lactis*, which is inhibited by intracellular phosphate [30]. Phosphate leakage was assumed to be negligible [30].

To simplify the model and reduce the number of parameters, some metabolites were lumped based on near-equilibrium timescale separation: (a) Glc6*P* and fructose 6-phosphate were placed in the Glc6*P* pool, (b) dihydroxyacetone phosphate and GA3P were placed in the GA3P and dihydroxyacetone (triose-P) pool, (c) 2-phosphoglycerate (2-PGA), 3-phosphoglycerate (3-PGA) and phospho*enol*pyruvate were placed in the phospho*enol*pyruvate pool and (d) all mixed-acid products (formate, ethanol and acetate) were placed in a single mixed-acids pool. The last choice is justified by the fact that under the conditions for which we developed the model, mixed-acid formation was negligible, as accounted for by the fact that the lactate concentration measured in the medium at the end of the experiments corresponded to approximately double the concentration of glucose entered (Fig. 2). The ATP/ADP, NAD^+/NADH and P_i pools are set as free-state variables, in contrast to other kinetic models [14,31,32]. Fig. 3A shows the structure of the *L. lactis* model.

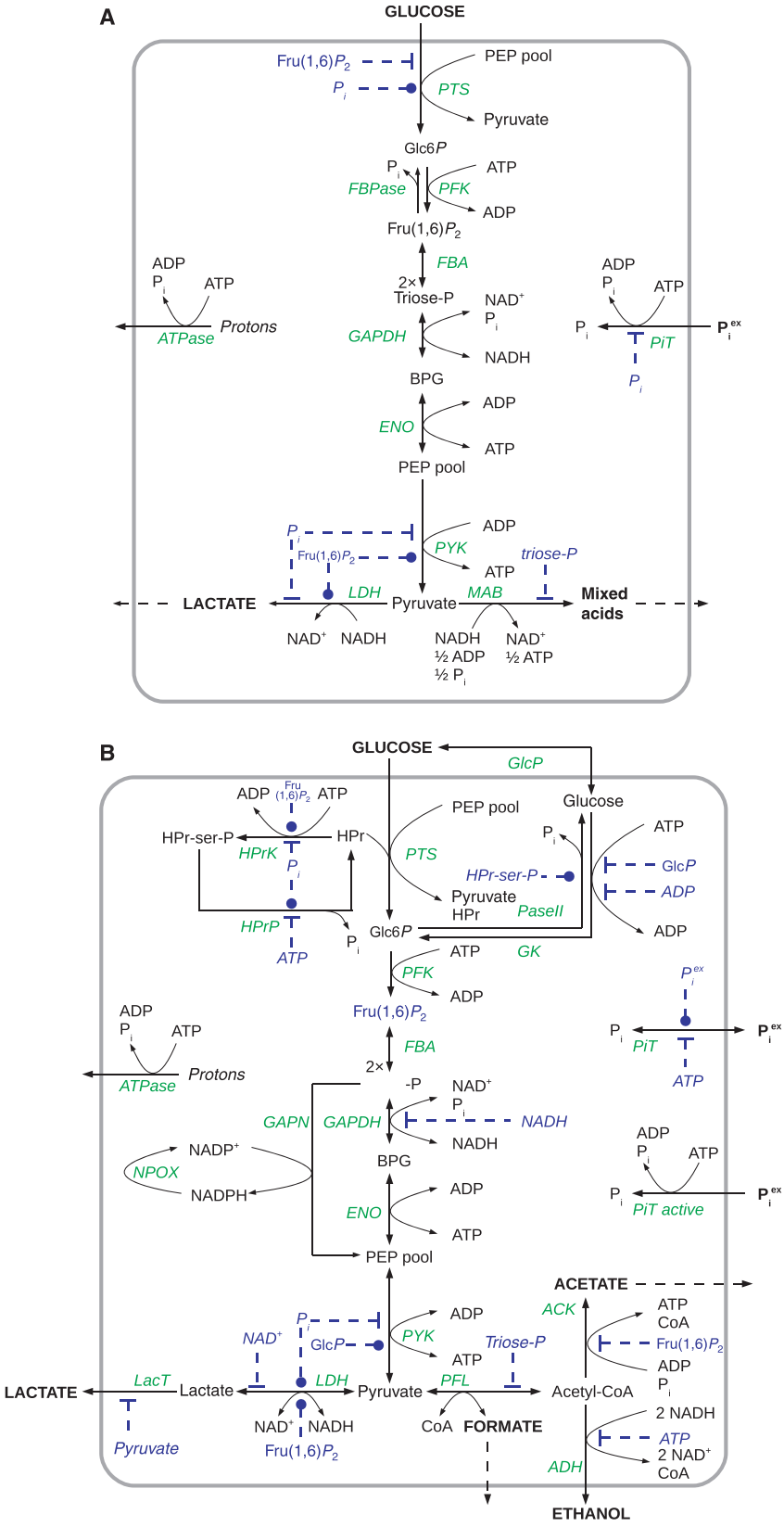

Fig. 3. Overview of molecular interactions of (A) *Lactococcus lactis* and (B) *Streptococcus pyogenes* glycolysis. Allosteric regulation (blue) is divided in inhibition (barred arrows) or activation (open circle-ends). Enzymes are given in green. BPG, 1,3-bisphosphoglycerate; ENO, enolase; FBA, fructose-1,6-bisphosphate aldolase; FBPase; fructose-1,6-bisphosphate phosphatase; GlcP, glucose permease; HPrK, HPr kinase; HPrP, HPr phosphatase; LacT, lactate transporter; MAB, mixed acid branch; NPOX, $NADP^+$ regenerating reaction; PEP, phospho*enol*pyruvate; PFL, pyruvate formate lyase; PFK, phosphofructokinase; PiT, phosphate transporter; PYK, pyruvate kinase.

The parameters in the model were optimized with parameter estimation to fit *in vivo* time-series data (see Tables S1–6 for the parameters and the Materials and methods for more information on the fitting procedure). These time-series data comprised our own measurements (Fig. 2) as well as the NMR data published by Neves *et al.* [17] (Fig. 4). For the two different data sets, the initial concentrations of metabolites (both measured and fitted) were allowed to differ, as was the activity of the ATPase. In addition, the initial concentrations that were not measured in our own or in the respective NMR data were fitted for our own data sets or the respective data sets of Neves *et al.* Thus, the initial concentrations of phospho*enol*pyruvate, extracellular lactate, ATP (without phosphate in the medium), ADP, intracellular phosphate and NAD were fitted for our experiments (at 10 and 50 mM extracellular phosphate). For the data of Neves *et al.*, the initial concentrations of ATP, ADP and phosphate for the ^{13}C-NMR data set and of Fru(1,6)P_2, lactate, NAD, phospho*enol*pyruvate and ADP for the ^{31}P-NMR data set were fitted. All other parameters stayed the same, irrespective of the assumption that the V_{max} values (that include the enzyme expression levels) for the two different experimental data sets will certainly not be exactly the same. However, the model with these constraints is able to fit the data almost perfectly as long as phosphate uptake is included in the model. Without this reaction, the data cannot be fitted.

As the experimental data do not allow an unambiguous fit of the data and the parameters are not identifiable (between the different fits, all parameters varied over a wide range within the set boundaries), we performed 300 fits and subjected the best 50 (based on the objective value and visual inspection) to the analysis below in order to ensure that we were observing robust effects that do not depend on the exact choice of the parameters.

In summary, it is clear that P_i exchange plays an important role in sustaining a large intracellular total P_i pool, affecting the levels of phosphorylated metabolic intermediates. This *L. lactis* model (Fig. 3A and Tables S1–S6) subsequently formed a scaffold for the first kinetic model of *S. pyogenes* glycolysis (Fig. 3B and Tables 7–12).

Setting up the *S. pyogenes* model using *L. lactis* as a blueprint

The primary metabolism of *S. pyogenes* largely resembles that of *L. lactis* with respect to allosteric regulation and general enzyme characteristics. A few additional enzymes are present, as indicated later. Our measurements of the kinetics of pyruvate kinase of *S. pyogenes* and LDH showed differences in allosteric regulation by phosphate and Glc6*P*, respectively (see Table S10). Finally, our experimental data uncovered that *S. pyogenes* has a larger heterofermentative capac-

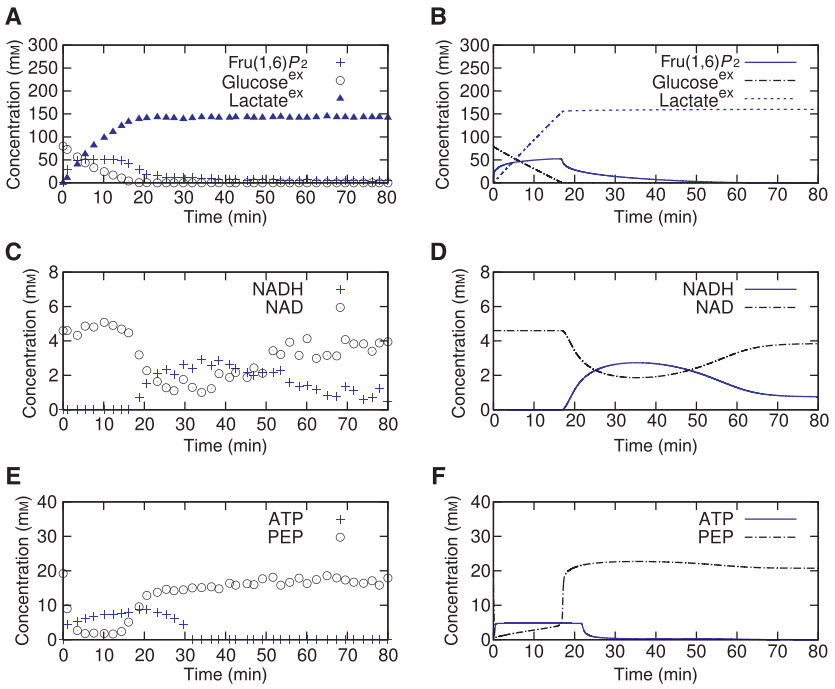

Fig. 4. Metabolic profiles and model simulations of glucose-pulse experiments in *Lactococcus lactis*. ^{13}C- and ^{31}P-NMR time-series profiles [17] of (A) Fru(1,6)P_2, glucose and lactate, (C) NAD^+ and NADH, and (E) the phospho*enol*pyruvate (PEP) pool and ATP when 80 mM glucose is added; (B), (D) and (F) are corresponding model simulations of the *L. lactis* model. The simulations were performed with an intracellular to extracellular volume ratio of 0.047; the initial concentrations for both ^{13}C- and ^{31}P-NMR experiments are given in Table S6.

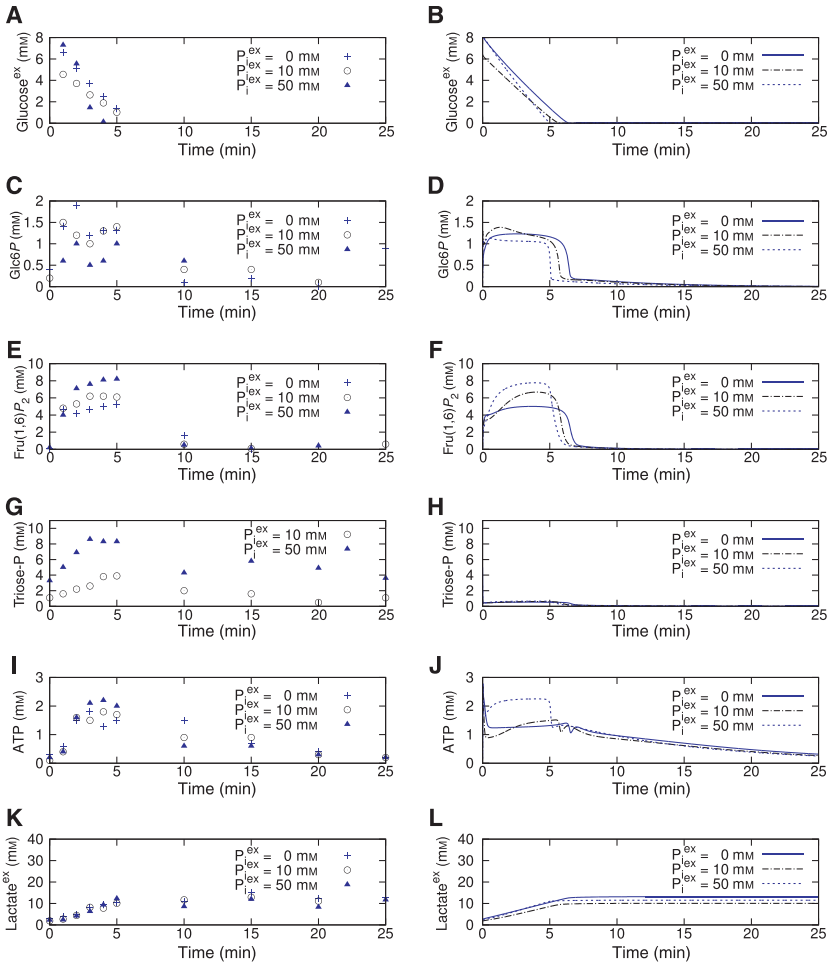

Fig. 5. Experimental data and model simulations of 6 and 8 mM glucose-pulse experiments in *Streptococcus pyogenes*. We measured the influence of 0 mM (crosses), 10 mM (circles) and 50 mM (triangles) extracellular P_i on the dynamics of (A) extracellular glucose, (C) Glc6*P*, (E) Fru(1,6)P_2, (G) triose-P, (I) ATP and (K) extracellular lactate. Simulations show similar quantitative trends in (B), (D), (F), (H), (J) and (L), respectively. For the simulations, the intracellular to extracellular volume ratio was fixed to 0.036, 0.0321 and 0.0348, respectively. The initial concentrations for all extracellular phosphate concentrations are given in Table S12.

ity than *L. lactis* [11]. Thus, as shown in Fig. 5, the experimentally observed accumulated lactate levels do not represent twice the amount of glucose entered. This motivated a more detailed description of the mixed-acid branch for the *S. pyogenes* model.

We transformed the *L. lactis* model into a *S. pyogenes* model by including or changing the following. (a) Decomposition of PTS to a low-molecular-weight, heat-stable protein (HPr) and serine-phosphorylated HPr (HPr-ser-P), including regulation by Fru(1,6)P_2, P_i and ATP [33,34]. This was motivated by (b) removal of fructose-1,6-bisphosphatase (EC 3.1.3.11) as the gene for this enzyme is not present in the genome. Instead, an expulsion mechanism of Glc6*P* was introduced, which is catalyzed by the HPr-ser-P-activated sugar-phosphate phosphatase II (PaseII; EC 3.1.3.23) [35]. (c) Inclusion of a glucose permease that removes some of the glucose produced from dephosphorylated Glc6*P* by PaseII and a glucokinase (EC 2.7.1.2), which is allosterically inhibited by Glc6*P* and ADP [36]. (d) Incorporation of the nonphosphorylating $NADP^+$-dependent glyceraldehyde-3-phosphate dehydrogenase (GAPN; EC 1.2.1.9). This GAPN catalyses the irreversible conversion of GA3P to 3-PGA by reducing $NADP^+$ to NADPH. As the oxidative part of the pentose phosphate pathway is missing in *S. pyogenes*, it functions as an alternative mechanism for the production of NADPH [37]. Additionally, an $NADP^+$-regenerating reaction is introduced. (e) Changing pyruvate kinase activation by Fru(1,6)P_2 into Glc6*P* [38] and adding NADH inhibition of glyceraldehyde-3-phosphate dehydrogenase (GAPDH; EC 1.2.1.12) [39]. (f) Allosteric regulation of LDH by NAD^+ (inhibition) and Fru(1,6)P_2 and P_i (both activation), which we determined experimentally (Table S10). (g) Pyruvate-controlled export of lactate [40] and (h) division of the mixed-acid branch in acetate and ethanol production and inclusion of an allosteric inhibition of Fru(1,6)P_2 and ATP, respectively [41,42].

Finally, with the analysis of the experimental data in mind, we investigated the mechanism of P_i uptake in

S. pyogenes. Based on the experimental findings we incorporated facilitated diffusion of P_i, which is inhibited by ATP and activated by extracellular phosphate [43] and, additionally, ATP-dependent uptake of P_i [44]. Figure 3B gives a schematic overview of the molecular interactions of the *S. pyogenes* glycolysis model.

Like the *L. lactis* model, the *S. pyogenes* model needed additional parameter fitting to simulate the profiles of our *in vivo* experimental data. Again, the model is able to fit the experimental data (Fig. 5), as long as the phosphate-uptake system is in place. However, and again, the parameters are underdetermined and the resulting parameter set is not unique. Therefore, and similarly to the *L. lactis* model, we repeated fitting 300 times and analysed the best 50 fits subsequently. The parameters of the *S. pyogenes* model are listed in Tables S7–S12.

Comparative systems biology of *L. lactis* and *S. pyogenes* glycolysis

The uptake of P_i in *L. lactis* and *S. pyogenes* proceeds via active transport [30,44] and in *S. pyogenes* also via facilitated diffusion [43]. As described earlier, our glucose-pulse experiments in resting cells with different concentrations of extracellular P_i (0, 10 and 50 mM) showed that the levels of Fru(1,6)P_2 in both species are affected by the extracellular P_i concentration. This is reflected and reproduced by our kinetic models. Although a slightly different set of initial conditions is used for each perturbation in extracellular P_i in order to fit the slightly different experimental conditions, we verified the impact of the external P_i concentration within each model by simulating the Fru(1,6)P_2 level and the glucose-uptake rate with varying external concentrations of P_i and left the remaining initial concentrations unchanged. Therefore, we conclude that the observed effects are caused by responses to external conditions and not by different initial concentrations. The experiments were reproduced several times with an exemplary data set displayed in Figs 2 and 5.

The rate of glucose uptake was also slightly altered by extracellular P_i in *L. lactis* and to a greater extent in *S. pyogenes* (Figs 2A and 5A) with glucose-uptake rates that were higher in *S. pyogenes* than in *L. lactis*. Once again, our models reproduce this behaviour very well (see Figs 2B and 5B). Interestingly, the glucose-uptake rate in *S. pyogenes* did not simply correlate with the extracellular phosphate concentration. Rather, in the simulations of the model with the indicated parameters, low extracellular phosphate concentrations (e.g. around 1 mM) decreased the glucose uptake slightly compared with no phosphate in the environment, whereas higher phosphate concentrations increased the glucose uptake rate (see Fig. 6). This observation is not easy to explain. Because free phosphate has such a pronounced effect on glycolysis and glucose uptake, we studied the behaviour of intracellular phosphate in our model. Intracellular phosphate is extremely difficult to determine experimentally in the presence of extracellular phosphate. Insights from computational models are therefore advantageous. Curiously, we observed that the intracellular phosphate level in *L. lactis* simply increases with increasing extracellular levels of phosphate, but this does not hold for *S. pyogenes* (Fig. 6). As mentioned before, both bacteria possess an ATP-dependent phosphate-uptake system. *S. pyogenes* also has an energy-independent phosphate transporter that is modelled as facilitated diffusion and is inhibited by ATP and activated by extracellular phosphate [43]. Hereby, the net uptake is determined by the difference in the extracellular and intracellular phosphate levels, which implies that an efflux of phosphate occurs if the intracellular phosphate concentration is higher than the extracellular level and some external phosphate is present. Therefore, owing to the combination of active and passive phosphate transport, a low concentration of extracellular phosphate can lead to a small decrease of intracellular phosphate in *S. pyogenes*, if the concentration gradient is pointing to the outside of the cell. Figure 6 displays a parameter scan of intracellular phosphate against extracellular phosphate as well as the effect of extracellular phosphate on the flux through the passive phosphate transport system for *S. pyogenes*. For a low extracellular phosphate level (e.g. around 1 mM), the flux through the phosphate transporter is directed towards the outside, removing phosphate from the cytosol, whereas higher phosphate concentrations result in phosphate uptake. Thus, it is obvious that certain low concentrations of extracellular phosphate lead to a decreased concentration of intracellular phosphate compared with no extracellular phosphate. In turn, intracellular phosphate activates the PTS and is an important substrate for GAPDH and acetate kinase (EC 2.7.2.1). Therefore, a decreased concentration of intracellular phosphate leads to a decreased glucose-uptake rate.

Because of the nonidentifiability of the parameters, we studied the 50 best fits of *S. pyogenes* with respect to this behaviour. The behaviour reported above was the same in many ($\sim$ 60%) of the fits, but not in all. As an example, Fig. 7 shows the dependency of the PTS flux on the initial extracellular phosphate concentration for both organisms and for different parameter

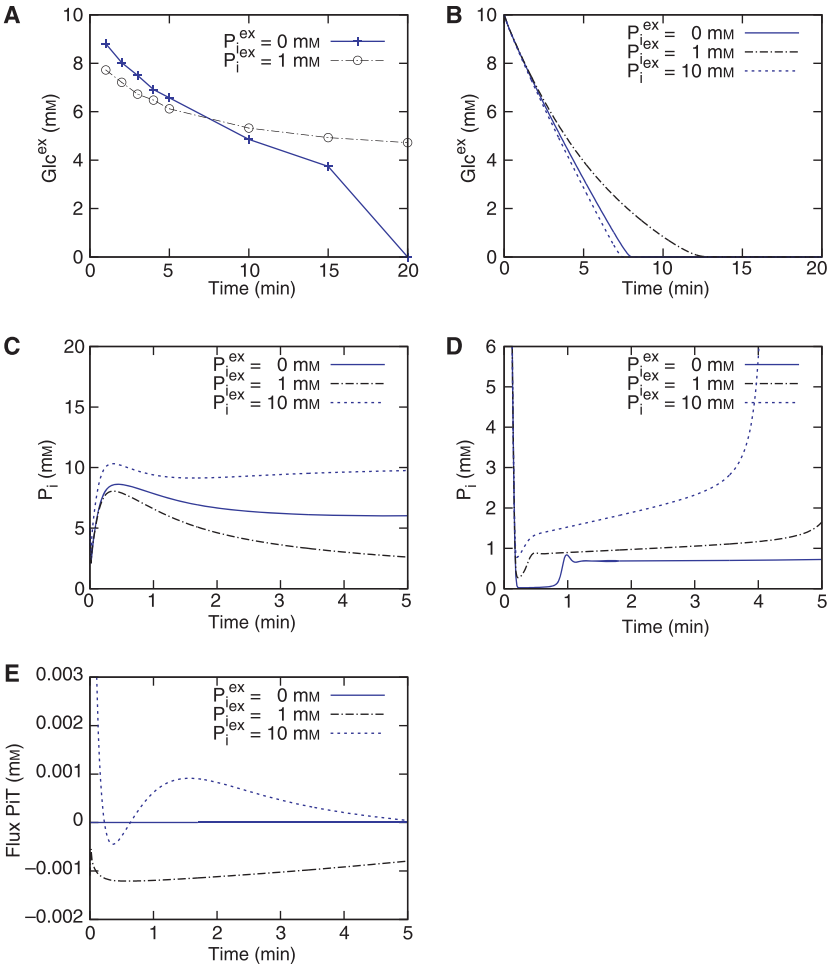

Fig. 6. Metabolic profiles and the first minutes of model simulations of 10 mM glucose-pulse experiments in *Streptococcus pyogenes* and *Lactococcus lactis*. Our model predicts that low extracellular P_i concentrations decrease glucose uptake in *S. pyogenes*, which we could validate experimentally (A); model simulations are shown in (B). We observe that low extracellular P_i concentrations (such as 1 mM) decrease the internal phosphate level in *S. pyogenes* (C), whereas intracellular phosphate increases with the extracellular level in *L. lactis* (D). Owing to the presence of a passive phosphate transporter (PiT) in *S. pyogenes*, low extracellular phosphate concentrations result in phosphate efflux (E) and thus decrease the intracellular phosphate concentration. As the PTS system is regulated by phosphate, the sugar uptake is slower at low extracellular phosphate concentrations. This is not the case in *L. lactis*, which demonstrates active phosphate uptake. Here, even low extracellular phosphate concentrations increase the intracellular level (results not shown).

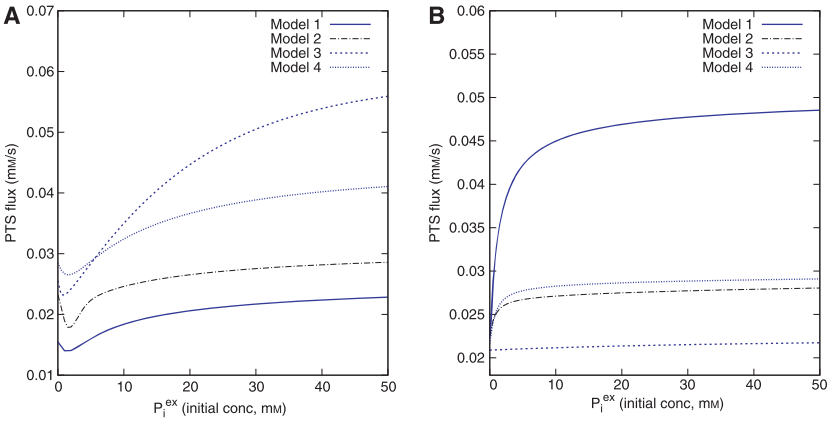

Fig. 7. Dependency of the PTS flux on the initial concentration of extracellular phosphate in (A) *Streptococcus pyogenes* and (B) *Lactococcus lactis* for four fitted models. It is obvious that a low initial external phosphate level decreases the PTS flux, and thus the sugar uptake, in *S. pyogenes* but has no effect on glucose uptake in *L. lactis*.

sets, which all resulted in a reasonable fit of the experimental data. Obviously, there are differences in the quantitative behaviour. However, the qualitative behaviour is the same. As this behaviour is not completely robust in all of the fits, it is obviously crucial to verify experimentally the observations resulting from this analysis. The effect on glucose uptake was also observed experimentally and the respective data (which were not used for fitting of the model) are also shown in Fig. 6. The validation showed that the computationally predicted behaviour indeed coincided qualitatively with the experimental results. The experimentally

observed effect was even more pronounced than the computationally predicted effect.

We performed additional *in silico* experiments with our kinetic models of *S. pyogenes* and *L. lactis*, in which extracellular glucose and phosphate levels were varied. Our experimental fermentation studies showed that glucose uptake in *S. pyogenes* ceases when extracellular glucose levels rise above 20 mM under the experimental conditions employed. We observed that *S. pyogenes* consumes 5–10 mM of the pulse and subsequently stops sugar uptake. In contrast to *S. pyogenes*, extracellular glucose levels of ≥ 20 mM do not hinder glucose uptake in *L. lactis*. We therefore varied the amount of extracellular glucose in our simulation for all fitted parameter sets in the models of *L. lactis* and *S. pyogenes*. In all models, if no or low external phosphate was present for *S. pyogenes*, the glucose uptake was completely stopped or severely inhibited at high glucose levels (the exact numerical value varied between the different fits). Often the actual value was much higher (and nonphysiological) compared with the experimental set-up (ranging between 113 mM and 89 M), but qualitatively this was robust behaviour irrespective of the exact parameter set. This effect could also be seen in several of the models for *L. lactis*, but at even higher external glucose concentrations (between 40 mM and 95 M). Once again, this inhibition could be overcome by adding phosphate, underlining again the crucial importance of this substance for glucose uptake and glycolysis in general.

Discussion

The goal of this study was to apply a comparative systems biology approach to investigate glycolysis in two closely related lactic acid-producing bacteria that live in nutrient-rich, but rather distinct, environments. First of all, we formulated a kinetic model of *L. lactis* glycolysis, which was able to capture, with improved accuracy, dynamic profiles of intracellular metabolites after glucose-pulse experiments. Previous models of *L. lactis* glycolysis did not quantitatively fit the NMR data of Neves *et al.* [17,23,31]. Incorporation of the effects of extracellular P_i on the intracellular phosphorylated glycolytic intermediates was found to be key. It should be noted that Neves *et al.* [17], in the Materials and methods section of their study, mentioned that they observed no difference in the Fru(1,6)P_2, phospho*enol*pyruvate and 3-PGA levels when using a phosphate-free buffer compared with the published time-series with 50 mM external phosphate. We are not able to explain this finding here since the earlier described obvious phosphate uptake during glucose consumption in their experiments should result in differences in phosphorylated compounds when no phosphate is available. Our own experimental data showed a clear dependency with respect to external phosphate. Perhaps the distribution of differences in phosphorylated compounds in their strain (which was different from that used in the present study) was somewhat different and difficult to observe.

All previously published models omitted P_i transport [12,13,15,16] or considered P_i as a constant input [14,31,32]. Consequently, the simulated Fru(1,6)P_2 and intracellular P_i levels were considerably lower in these studies, which affected the regulation of many glycolytic processes, amongst which are PTS [24], pyruvate kinase [26] and LDH [45]. Our *L. lactis* model is the first to (a) quantitatively describe the dynamics of extracellular metabolites (glucose and lactate), the main glycolytic intermediates (Fru(1,6)P_2, Glc6P and phospho*enol*pyruvate) and cofactors (ADP/ATP, NAD^+/NADH and P_i), (b) fit the dynamics for different strains (i.e. MG1363 for the Neves experiments [17] and NZ9000, a MG1363 derivative, for our glucose-pulse experiments) with one single thermodynamically consistent parameter set (although with variable ATPase activities) and (c) take into account the effects of varying amounts of extracellular phosphate. In particular, the high Fru(1,6)P_2 concentration during glycolysis appeared to be crucial for the regulation of several glycolytic enzymes and the glucose-uptake rate, and was a direct result of the extracellular phosphate concentration.

It should be noted that in glycolytic models of most other organisms, P_i is rarely a free metabolite (e.g. yeast [46]). This is actually surprising in view of the many effects of phosphate on enzyme kinetics and as a result of the fact that phosphate is a factor which determines the free-energy of ATP hydrolysis (being its product). Classical experiments by Harden and Young, in yeast extracts, have already demonstrated the importance of phosphate for glycolytic flux [47,48]. Our study suggests and reinforces the fact that major improvements can be made by studying phosphate dynamics more carefully in all organisms.

The structure and modelling framework of *L. lactis* served as a scaffold for the first kinetic model of *S. pyogenes* glycolysis to reduce the amount of man-hours needed for such an effort. Furthermore, it strongly facilitates interspecies comparisons. We adapted the model structure of *L. lactis*, acquired kinetic details of LDH and performed glucose-pulse experiments to optimize the model of *S. pyogenes*. Interestingly, our LDH kinetics measurements indicated allosteric activation of LDH by P_i in *S. pyogenes*, which is

significantly different from *L. lactis*. Despite little knowledge about *S. pyogenes*, we developed a model that was able to describe our experimental data quantitatively, except for the triose-P level, which in our simulations was lower than the experimentally determined level. This might have been caused by placing metabolites in pools in our computational model.

On the one hand, our comparative systems approach helped to develop a model for a less commonly studied organism (*S. pyogenes*) based on the knowledge of a closely related well-described lactic acid bacteria (*L. lactis*) but, on the other hand, this might also lead to a certain bias when comparing the species. The model was constructed by incorporating known differences between both species (i.e. distinct phosphate uptake, regulation and parametrization). Therefore, differences between the two models must have been caused by the introduced variance. We were able to explain the differences observed in our experiments just by taking these identified biochemical differences into account, which is certainly interesting, but obviously there might be more, so far unidentified, differences that add to this picture.

The role of phosphate is crucial in both organisms, even though uptake and regulation show some differences. Experimental approaches showed that an increase in the extracellular phosphate concentration induced an elevation in Fru(1,6)P_2 in both species and an increased glucose-uptake rate in *S. pyogenes*. In the latter, the relationship of extracellular phosphate concentration and glucose uptake is not monotonic. Rather, we find that a low extracellular phosphate concentration can actually hamper glucose uptake, whereas high concentrations stimulate it. This is not the case in *L. lactis* and we could ascribe this difference in behaviour mainly to the differences in phosphate-uptake mechanisms because passive transport (even well-regulated passive transport) will allow phosphate efflux if the concentration gradient points in this direction. In *S. pyogenes*, phosphate uptake also seems to prevent a stalling of glucose metabolism at high glucose concentrations. This is also seen in our model simulations without any additional parameter fitting: when no phosphate is provided extracellularly, *S. pyogenes* fails to consume all glucose but this process is stalled before the glucose is fully consumed. Owing to the nonidentifiability of the kinetic parameters in our models with the current set of experimental data, it is important to note here that the observed computational results are robust and resulted from an analysis of 50 different parameter fits.

Having revealed the fundamental role of free phosphate for the metabolism of these species, it is interesting to see how the two bacteria cope with the phosphate available in their respective natural environment. *S. pyogenes*, which is present in the human body (e.g. on skin and mucous membrane and in blood (0.8–1.8 mM P_i in the latter)) at relatively constant and low concentrations of phosphate, has passive and active phosphate-uptake mechanisms. Both have to supply sufficient phosphate to the cells to enable them to metabolize glucose efficiently in order to grow and multiply. However, according to the above, the relatively low phosphate concentrations are not optimal conditions for glucose uptake by this organism. This raises the question of why *S. pyogenes* still uses the passive transport mechanism. The answer might lie in the fairly constant supply of phosphate and glucose in the compartments of the human body. Thus, while not allowing optimal glucose-uptake rates, the passive transport system permits a cheap and guaranteed uptake of minimal phosphate (the phosphate concentration in its natural environment will certainly never drop much) that is sufficient to sustain glycolysis. Interestingly, only recently has the putative gene sequence of a sodium phosphate symporter been reported for *S. pyogenes* (see accession number B5XHT4 in UniProt [49]).

L. lactis, on the other hand, initially encounters relatively high phosphate levels ($\sim$ 20 mM) in fresh milk. However, here, the situation is similar to batch experiments in that there is no further supply of phosphate in the milk once it has left the body and *L. lactis* starts to reside in it. Thus, an active mechanism, as found for phosphate uptake in these bacteria, makes sense, even though one may wonder why the bacteria do not have a passive transporter that would allow them to make use of the initially high phosphate concentration without wasting ATP. As seen for *S. pyogenes*, a passive transporter can slow down glucose uptake if the extracellular phosphate concentration starts to deplete. This might be dangerous for a species that encounters highly variable environmental conditions. For *L. lactis*, no putative sodium phosphate symporter has so far been identified. Sugar uptake is activated by intracellular phosphate in both organisms but is stimulated more strongly by extracellular phosphate in *S. pyogenes* than in *L. lactis*. This was also observed in the experimental data.

Another interesting difference is that *S. pyogenes* possesses an $NADP^+$-dependent GAPDH (GAPN) that is not present in the genome of *L. lactis*. Although initially introduced to produce NADPH for biosynthesis (recall that *S. pyogenes* lacks an oxidative part of the pentose phosphate pathway), this reaction enables *S. pyogenes* to produce phospho*enol*pyruvate required for sugar uptake in the absence of phosphate. This

may compensate slightly for the unfavourable low external phosphate concentrations. Indeed, removing the $NADP^+$-dependent GAPDH reaction from our model led to a much stronger reduction of glucose uptake at low external phosphate concentrations.

Another interesting observation is the fact that *S. pyogenes* seems to be more efficient in converting glucose to ATP, while exhibiting a higher glucose-uptake rate, than *L. lactis*. The model shows this to be a direct consequence of the antagonistic effects of allosteric regulators (Fru(1,6)P_2, P_i, NAD^+ and NADH). Pyruvate kinase and especially LDH are differently regulated in *L. lactis* (Fig. 3A) and *S. pyogenes* (Fig. 3B). In *L. lactis*, LDH is allosterically regulated by Fru(1,6)P_2 and antagonistically regulated by P_i, indicating that during glycolysis where P_i is low and Fru(1,6)P_2 is high, the flux is directed towards the less efficient lactate production. *S. pyogenes* LDH lacks this antagonistic regulation by Fru(1,6)P_2 and P_i. Here, both Fru(1,6)P_2 and P_i activate LDH, whereas the product NAD^+ inhibits LDH. This indicates that LDH activity is submaximal during glycolysis and more flux can be diverted to the more efficient mixed-acid fermentation.

The above observations on the phosphate regulation of LDH are corroborated at the kinetic level by the differences between plant and dairy strains of *L. lactis*. Van Niel *et al.* [27] measured that LDH activity is differentially regulated in plant and dairy strains of *L. lactis*: dairy strains use Fru(1,6)P_2 and P_i, whereas the LDHs of plant isolates are regulated by the $NADH/NAD^+$ ratio. As a plant environment is virtually devoid of phosphate [50], these observations support a close link between the organism's natural environment and its metabolic regulation.

To summarize, our comparative systems biology approach resulted in (a) an improved kinetic model for *L. lactis*, (b) an acceleration of the development of the first kinetic model of the pathogenic *S. pyogenes* for which very limited metabolic information was available and (c) insight into the crucial role of P_i transport and P_i regulation of glycolysis, which we could relate to the P_i availability in the environmental niches of these organisms. We expect that comparative approaches at the systems level will significantly enhance our understanding of the function of biological networks.

Materials and methods

Mathematical models of *L. lactis* and *S. pyogenes*

Mathematical models were formulated using ordinary differential equations, as specified in Data S1–S4 in Supporting information. Simulations were performed with the LSODA algorithm, as implemented in COPASI [51].

For both models, we performed an extensive literature search in the SABIO-RK and BRENDA databases [52,53] for enzyme-specific activities. From the measured dry weight of our experiments, the fact that 42% of cellular dry weight consists of protein [54] and an assumed intracellular to reactor volume ratio of 30 $mL \cdot L^{-1}$, we were able to calculate V_{max} values from the specific activities taken from Even *et al.* and Rimpiläinen *et al.* [55,56] (see also Tables S1 and S7). For the Michaelis constants, we took the values from previously published kinetic models [12,16], and regulator binding constants [26–28] and Hill coefficients [16] from previous publications. These values were used as initial estimates for parameter estimation (discussed later). For *S. pyogenes*, only kinetic constants of PaseII and the phosphate transporter were found in the literature [35,43]. For pyruvate kinase and LDH, the results from our own experiments were used. Most of the Michaelis constants were derived from enzymes of related organisms found in the literature [13,34,36,40,43,57–64], for example, from *Streptococcus mutans* or *Streptococcus thermophilus*. If no information was available, we adopted the missing parameters from the *L. lactis* model. Enzyme-specific activities were converted into V_{max} values as described for *L. lactis*. V_{max} values were derived from previous publications [13,35–37,39,43,57–59,62–65].

For both species, we implemented kinetic rate equations as convenience kinetics [66,67]. The equilibrium constants for the glycolytic reactions are known and were taken from the literature [16]. The rate equations, parameter values and additional information about the initial conditions are provided in the Supporting information.

As *in vitro* measurements can deviate considerably from *in vivo* conditions [46], and not all kinetic parameters were determined in *L. lactis* or *S. pyogenes*, we used parameter fitting methods to tune the parameters to match the time-series data for various concentrations of extracellular P_i. For both organisms, parameters found in the literature were used as initial guess and were allowed to vary between -90% and +900% of their initial values. Unknown parameters were modified over an even larger range (i.e. binding constants were varied from 0.01 to 100 mM and V_{max} values from 0.1 to 10^3 $mM \cdot s^{-1}$). To correct the volume of multicompartment reactions, the transport reactions have to be multiplied by a correction factor. In our models this factor was incorporated in the velocity constants of the transport reactions. Therefore, the range for these V_{max} values was wider (0.001–1000 $mM \cdot s^{-1}$).

Subsequently, the Neves data [17] for *L. lactis* and our fermentation experiments for both organisms were used as input for a parameter estimation using the particle swarm algorithm (swarm size = 100), as implemented in COPASI [51].

Fermentation experiments

L. lactis cells were grown anaerobically at 37 °C in CDM-LAB medium [11,68] which contains (per liter): 1 g of K_2HPO_4, 5 g of KH_2PO_4, 0.6 g of ammonium citrate, 1 g of acetate, 0.25 g of tyrosine, 0.24 g of alanine, 0.125 g of arginine, 0.42 g of aspartic acid, 0.13 g of cysteine, 0.5 g of glutamic acid, 0.15 g of histidine, 0.21 g of isoleucine, 0.475 g of leucine, 0.44 g of lysine, 0.275 g of phenylalanine, 0.675 g of proline, 0.34 g of serine, 0.225 g of threonine, 0.05 g of tryptophan, 0.325 g of valine, 0.175 g of glycine, 0.125 g of methionine, 0.1 g of asparagine, 0.2 g of glutamine, 10 g of glucose, 0.5 g of L-ascorbic acid, 35 mg of adenine sulfate, 27 mg of guanine, 22 mg of uracil, 50 mg of cystine, 50 mg of xanthine, 2.5 mg of D-biotin, 1 mg of vitamin B_{12}, 1 mg of riboflavin, 5 mg of pyridoxamine-HCl, 10 μg of *p*-aminobenzoic acid, 1 mg of pantothenate, 5 mg of inosine, 1 mg of nicotinic acid, 5 mg of orotic acid, 2 mg of pyridoxine, 1 mg of thiamine, 2.5 mg of lipoic acid, 5 mg of thymidine, 200 mg of $MgCl_2$, 50 mg of $CaCl_2$, 16 mg of $MnCl_2$, 3 mg of $FeCl_3$, 5 mg of $FeCl_2$, 5 mg of $ZnSO_4$, 2.5 mg of $CoSO_4$, 2.5 mg of $CuSO_4$ and 2.5 mg of $(NH_4)_6Mo_7O_{24}$. *S. pyogenes* cells were grown in THY medium. This medium consists of 36.4 $g{\cdot}L^{-1}$ of Todd-Hewit Broth (Oxoid, Basingstoke, UK) and 5 $g{\cdot}L^{-1}$ of yeast extract (Oxoid).

Cells grown to mid-exponential phase were harvested by centrifugation at 4068 ***g*** for 10 min at room temperature, washed twice with 50 mM Mes buffer (pH 6.5) and finally suspended in the indicated buffer solution. Anaerobic conditions were established by flushing with nitrogen for 10 min. Glucose was added, and 400-μL samples were taken at regular time intervals and mixed immediately with 200 μL of a cold perchloric acid (3.5 M) solution. The extracts were kept on ice for maximally 60 min. The pH was neutralized with 160 μL of 2 M KOH. The pH-adjusted samples were centrifuged and the supernatants were stored at −80 °C for subsequent analysis. All metabolites were quantified by enzymatic methods coupled to the spectrophotometric determination of NAD(P)H.

Kinetic analysis of LDH of *S. pyogenes*

For heterologous expression of the LDH of *S. pyogenes*, chromosomal DNA of an M49 serotype strain was isolated according to the Qiagen Blood and Tissue Kit (Qiagen, Hilden, Germany) and used as a template for PCR amplification with the Phusion™ High Fidelity PCR Kit (Finnzymes, Vantaa, Finland) and the forward/reverse primer pair 5′-AGATGTTTAGGATCCACTGCAACTAA ACAA-3′/5′-TCTCTTTTGGTCGACGTTTTTAGCAGC-3′. The resulting PCR fragment was ligated into the pASK-IBA2 vector (IBA GmbH, Göttingen, Germany) system via *Bam*HI and *Sal*I restriction sites. The recombinant vector was heat-shock transformed into $CaCl_2$-competent *Escherichia coli* DH5α cells. Correct insertion of the PCR product was confirmed by plasmid sequencing. For heterologous expression of the corresponding enzyme, recombinant *E. coli* strains were grown in 200 mL of Luria–Bertani (LB) medium at 37 °C under vigorous shaking. At an absorbance ($A_{600\ nm}$) of about 0.4, expression was induced by the addition of anhydrotetracycline (0.2 $\mu g{\cdot}mL^{-1}$) and growth of the bacteria was allowed for another 2–4 h. Then, the cells were harvested by centrifugation and the bacterial pellets were stored overnight at −20 °C, subsequently thawed, suspended in 1 mL of Buffer W (100 mM Tris/HCl, pH 8.0, 1 mM EDTA and 150 mM NaCl) and disrupted using a Ribolyzer. Cell debris was removed by centrifugation for 10 min at 13 000 ***g*** and 4 °C. Clear supernatants were diluted 1 : 10 with Buffer W and applied to StrepTactin sepharose (IBA GmbH) columns. After washing the sepharose three times with 10 mL of Buffer W, recombinant Strep-tagged protein was eluted with 6 × 0.5 mL of Buffer E (Buffer W including 2.5 mM desthiobiotin). Elution fractions were checked for recombinant protein by SDS/PAGE and western blots using Strep-Tag-specific antibodies.

For LDH activity measurements, protein concentrations in the purified recombinant protein fractions were determined using the Bradford method (Bio-Rad Protein Assay Kit; Bio-Rad, Munich, Germany). The standard assay for determination of LDH activity was carried out by adding 50 μL of protein solution, 25 μL of Fru(1,6)P_2 (20 mM) and 25 μL of NADH (6.75 mM) to 800 μL of sodium-phosphate buffer (50 mM, pH 6.8). The mixture was heated to 37 °C and the reaction was started by adding 100 μL of prewarmed (37 °C) sodium pyruvate (100 mM) to the reaction mixture. The LDH activity was assayed by measuring the decrease of NADH in the mixture at 340 nm in a spectrophotometer for 5 min. The conversion of 1 μmol of NADH (ε_{NADH} = 6220 $L{\cdot}mol^{-1}{\cdot}cm^{-1}$) to NAD^+ per minute was defined as one unit of LDH activity. The activity was expressed as U per mg of protein. For determination of K_m values and allosteric regulation, the standard assay was modified by using varying concentrations of P_i, sodium pyruvate, Fru(1,6)P_2, NADH, ATP and NAD^+. For determination of the K_m values for the reverse reaction, NADH and sodium pyruvate were replaced with varying concentrations of NAD^+ and L-lactate.

Kinetic analysis of pyruvate kinase of *S. pyogenes*

Kinetic measurements of *S. pyogenes* pyruvate kinase were performed in protein crude extracts. For this purpose, cells from 50 mL of an exponentially growing *S. pyogenes* culture

in CDM-LAB medium [11,68] were harvested by centrifugation. Bacteria were washed twice in 1 × NaCl/P_i (PBS), suspended in 1 × NaCl/P_i to an absorbance ($A_{600\ nm}$) of 10 and lysed with 100 U of Phagelysin C (PlyC) per ml for 15 min at 37 °C [69,70]. Subsequently, cell debris was removed by centrifugation (10 min, 15 000 g) and the supernatant was filter-sterilized by passing through a 0.22-μm pore-size filter. For the standard pyruvate-kinase assay, 20 μL of protein crude extract was mixed with 880 μL of prewarmed (37 °C) reaction buffer (120 mM cacodylic acid, 120 mM KCl, 12 mM ADP, 1.2 mM Fru(1,6)P_2, 30 mM $MgCl_2$, 0.18 mM NADH, 5 U·mL^{-1} LDH). The reaction was started by the addition of 100 μL of prewarmed (37 °C) phospho*enol*pyruvate (20 mM). The pyruvate kinase activity was assayed by measuring the decrease of NADH in the mixture at 340 nm in a spectrophotometer for 5 min. The conversion of 1 μmol of NADH (ε_{NADH} = 6220 L·mol^{-1}·cm^{-1}) to NAD^+ per minute was defined as one unit of pyruvate kinase activity. The activity was expressed as U per mg of protein. For determination of K_m values the concentrations of the respective substrates were modified in the standard assay.

Acknowledgements

This work was financially supported by SysMO-LAB (Systems Biology of Microorganisms – Lactic acid bacteria). Bas Teusink and Domenico Bellomo are also supported through the Kluyver Center for Genomics of Industrial Fermentation, funded by the Netherlands Genomics Initiative. The authors would like to thank A. Z. Andersen for providing the Berkeley Madonna files of the Andersen model, H. Santos & A. R. Neves for answering our questions regarding their NMR data and J. Snoep for fruitful discussions. Finally, we would like to thank Susanne Roth and Nadine Veith for extensive literature search on *S. pyogenes*.

References

1 Salminen S (2004) Lars Axelsson: Lactic Acid Bacteria: Classification and Physiology. In *Lactic Acid Bacteria: Microbiological and Functional Aspects* (Salminen S, von Wright A & Ouwehan AC, eds), pp. 1–66. Marcel Dekker, Inc., New York.

2 Castresana J (2001) Comparative genomics and bioenergetics. *Biochim Biophys Acta* **1506**, 147–162.

3 Elgar G, Sandford R, Aparicio S, Macrae A, Venkatesh B & Brenner S (1996) Small is beautiful: comparative genomics with the pufferfish (Fugu rubripes). *Trends Genet* **12**, 145–150.

4 Molenaar D, Bringel F, Schuren FH, de Vos WM, Siezen RJ & Kleerebezem M (2005) Exploring *Lactobacillus plantarum* genome diversity by using microarrays. *J Bacteriol* **187**, 6119–6127.

5 Rubin GM, Yandell MD, Wortman JR, Miklos GLG, Nelson CR, Hariharan IK, Fortini ME, Li PW, Apweiler R, Fleischmann W *et al.* (2000) Comparative genomics of the eukaryotes. *Science* **287**, 2204–2215.

6 Kant R, Blom J, Palva A, Siezen RJ & De Vos WM (2010) Comparative genomics of Lactobacillus. *Microb Biotechnol* **4**, 323–332.

7 Smid EJ & Hugenholtz J (2010) Functional genomics for food fermentation processes. *Annu Rev Food Sci Technol* **1**, 497–519.

8 Cunningham MW (2000) Pathogenesis of group A streptococcal infections. *Clin Microbiol Rev* **13**, 470–511.

9 Thompson J (1988) Lactic acid bacteria: model systems for in vivo studies of sugar transport and metabolism in Gram-positive organisms. *Biochemie* **70**, 325–336.

10 Thomas TD, Ellwood EC & Longyear VM (1979) Change from homo- to heterolactic fermentation by Streptococcus lactis resulting from glucose limitation in anaerobic chemostat cultures. *J Bacteriol* **138**, 109–117.

11 Fiedler T, Bekker M, Jonsson M, Mehmeti I, Pritzschke A, Siemens N, Nes I, Hugenholtz J & Kreikemeyer B (2011) Characterization of three lactic acid bacteria and their isogenic ldh deletion mutants shows optimization for YATP (cell mass produced per mole of ATP) at their physiological pHs. *Appl Environ Microbiol* **77**, 612–617.

12 Hoefnagel MHN, Starrenburg MJC, Martens DE, Hugenholtz J, Kleerebezem M, van Swam II, Bongers R, Westerhoff HV & Snoep JL (2002) Metabolic engineering of lactic acid bacteria, the combined approach: kinetic modelling, metabolic control and experimental analysis. *Microbiology* **148**, 1003–1013.

13 Hoefnagel MH, van der Burgt A, Martens DE, Hugenholtz J & Snoep JL (2002) Time dependent responses of glycolytic intermediates in a detailed glycolytic model of *Lactococcus lactis* during glucose run-out experiments. *Mol Biol Rep* **29**, 157–161.

14 Voit EO, Neves AR & Santos H (2006) The intricate side of systems biology. *Proc Natl Acad Sci USA* **103**, 9452–9457.

15 Oh E, Lu M, Park C, Oh HB, Lee SY & Lee J (2011) Dynamic modeling of lactic acid fermentation metabolism with *Lactococcus lactis*. *J Microbiol Biotechnol* **21**, 162–169.

16 Andersen AZ, Carvalho AL, Neves AR, Santos H, Kummer U & Olsen LF (2009) The metabolic pH response in *Lactococcus lactis*: an integrative experimental and modelling approach. *Comput Biol Chem* **33**, 71–83.

17 Neves AR, Ventura R, Mansour N, Shearman C, Gasson MJ, Maycock C, Ramos A & Santos H (2002) Is the glycolytic flux in *Lactococcus lactis* primarily controlled by the redox charge? Kinetics of NAD+ and

NADH pools determined *in vivo* by 13C NMR. *J Biol Chem* **277**, 28088–28098.
18 Kulaev I, Vagabov V & Kulakovskaya T (1999) New aspects of inorganic polyphosphate metabolism and function. *J Biosci Bioeng* **88**, 111–129.
19 Mijakovic I, Poncet S, Galinier A, Monedero V, Fieulaine S, Janin J, Nessler S, Marquez JA, Scheffzek K, Hasenbein S *et al.* (2002) Pyrophosphate-producing protein dephosphorylation by HPr kinase/phosphorylase: a relic of early life? *Proc Natl Acad Sci USA* **99**, 13442–13447.
20 Sutrina SL, Reizer J & Saier MH (1988) Inducer expulsion in *Streptococcus pyogenes*: properties and mechanism of the efflux reaction. *J Bacteriol* **170**, 1874–1877.
21 Mason PW, Carbone DP, Cushman RA & Waggoner AS (1981) The importance of inorganic phosphate in regulation of energy metabolism of *Streptococcus lactis*. *J Biol Chem* **256**, 1861–1866.
22 Melchiorsen CR, Jensen NB, Christensen B, Jokumsen KV & Villadsen J (2001) Dynamics of pyruvate metabolism in *Lactococcus lactis*. *Biotechnol Bioeng* **74**, 271–279.
23 Neves AR, Pool WA, Kok J, Kuipers OP & Santos H (2005) Overview on sugar metabolism and its control in *Lactococcus lactis* – the input from in vivo NMR. *FEMS Microbiol Rev* **29**, 531–554.
24 Deutscher J, Francke C & Postma PW (2006) How phosphotransferase system-related protein phosphorylation regulates carbohydrate metabolism in bacteria. *Microbiol Mol Biol Rev* **70**, 939–1031.
25 Castro R, Neves AR, Fonseca LL, Pool WA, Kok J, Kuipers OP & Santos H (2008) Characterization of the individual glucose uptake systems of *Lactococcus lactis*: mannose-PTS, cellobiose-PTS and the novel GlcU permease. *Mol Microbiol* **71**, 795–806.
26 Crow VL & Pritchard GG (1976) Purification and properties of pyruvate kinase from *Streptococcus lactis*. *Biochim Biophys Acta* **438**, 90–101.
27 van Niel EW, Palmfeldt J, Martin R, Paese M & Hahn-Hägerdal B (2004) Reappraisal of the regulation of lactococcal L-lactate dehydrogenase. *Appl Environ Microbiol* **70**, 1843–1846.
28 Asanuma N & Hino T (2000) Effects of pH and energy supply on activity and amount of pyruvate formate-lyase in *Streptococcus bovis*. *Appl Environ Microbiol* **66**, 3773–3777.
29 Solem C, Koebmann B & Jensen PR (2008) Control analysis of the role of triosephosphate isomerase in glucose metabolism in *Lactococcus lactis*. *IET Syst Biol* **2**, 64–72.
30 Poolman B, Nijssen RM & Konings WN (1987) Dependence of *Streptococcus lactis* phosphate transport on internal phosphate concentration and internal pH. *J Bacteriol* **169**, 5373–5378.
31 Neves AR, Ramos A, Nunes MC, Kleerebezem M, Hugenholtz J, de Vos WM, Almeida J & Santos H (1999) In vivo nuclear magnetic resonance studies of glycolytic kinetics in *Lactococcus lactis*. *Biotechnol Bioeng* **64**, 200–212.
32 Voit EO, Almeida J, Marino S, Lall R, Goel G, Neves AR & Santos H (2006) Regulation of glycolysis in *Lactococcus lactis*: an unfinished systems biological case study. *Syst Biol (Stevenage)* **153**, 286–298.
33 Deutscher J, Pevec B, Beyreuther K, Kiltz HH & Hengstenberg W (1986) Streptococcal phosphoenolpyruvate-sugar phosphotransferase system: amino acid sequence and site of ATP-dependent phosphorylation of HPr. *Biochemistry* **25**, 6543–6551.
34 Reizer J, Novotny MJ, Hengstenberg W & Saier MH (1984) Properties of ATP-dependent protein kinase from *Streptococcus pyogenes* that phosphorylates a seryl residue in HPr, a phosphocarrier protein of the phosphotransferase system. *J Bacteriol* **160**, 333–340.
35 Ye JJ, Minarcik J & Saier MHJ (1996) Inducer expulsion and the occurrence of an HPr(Ser-P)-activated sugar-phosphate phosphatase in *Enterococcus faecalis* and *Streptococcus pyogenes*. *Microbiology* **142**, 585–592.
36 Porter EV, Chassy BM & Holmlund CE (1982) Purification and kinetic characterization of a specific glucokinase from *Streptococcus mutans* OMZ70 cells. *Biochim Biophys Acta* **709**, 178–186.
37 Iddar A, Valverde F, Serrano A & Soukri A (2003) Purification of recombinant non-phosphorylating NADP-dependent glyceraldehyde-3-phosphate dehydrogenase from *Streptococcus pyogenes* expressed in *E. coli*. *Mol Cell Biochem* **247**, 195–203.
38 Yamada T & Carlsson J (1975) Glucose-6-phosphate-dependent pyruvate kinase in *Streptococcus mutans*. *J Bacteriol* **124**, 562–563.
39 Pancholi V & Fischetti VA (1992) A major surface protein on group A streptococci is a glyceraldehyde-3-phosphate-dehydrogenase with multiple binding activity. *J Exp Med* **176**, 415–426.
40 Harold FM & Levin E (1974) Lactic acid translocation: terminal step in glycolysis by *Streptococcus faecalis*. *J Bacteriol* **117**, 1141–1148.
41 Lopez de Felipe F & Gaudu P (2009) Multiple control of the acetate pathway in *Lactococcus lactis* under aeration by catabolite repression and metabolites. *Appl Microbiol Biotechnol* **82**, 1115–1122.
42 Palmfeldt J, Paese M, Hahn-Hägerdal B & Niel EWJV (2004) The pool of ADP and ATP regulates anaerobic product formation in resting cells of *Lactococcus lactis*. *Appl Environ Microbiol* **70**, 5477–5484.
43 Reizer J & Saier MH (1987) Mechanism and regulation of phosphate transport in *Streptococcus pyogenes*. *J Bacteriol* **169**, 297–302.
44 Ferretti JJ, McShan WM, Ajdic D, Savic DJ, Savic G, Lyon K, Primeaux C, Sezate S, Suvorov AN, Kenton S

et al. (2001) Complete genome sequence of an M1 strain of *Streptococcus pyogenes*. *Proc Natl Acad Sci USA* **98**, 4658–4663.
45 Castro R, Neves AR, Fonseca LL, Pool WA, Kok J, Kuipers OP & Santos H (2009) Characterization of the individual glucose uptake systems of *Lactococcus lactis*: mannose-PTS, cellobiose-PTS and the novel GlcU permease. *Mol Microbiol* **71**, 795–806.
46 Teusink B, Passarge J, Reijenga CA, Esgalhado E, van der Weijden CC, Schepper M, Walsh MC, Bakker BM, van DamK, Westerhoff HV *et al*. (2000) Can yeast glycolysis be understood in terms of in vitro kinetics of the constituent enzymes? Testing biochemistry. *Eur J Biochem* **267**, 5313–5329.
47 Harden A & Young WJ (1906) The alcoholic ferment of yeast-juice. *Proc R S B Biol Sci* **77**, 405–420.
48 Harden A & Young WJ (1908) The alcoholic ferment of yeast-juice, part III: the function of phosphates in the fermentation of glucose by yeast-juice. *Proc R Soc Lond B* **80**, 299–311.
49 UniProt Consortium (2010) The Universal Protein Resource (UniProt) in 2010. *Nucleic Acids Res* **38**, D142–D148.
50 Asher CJ & Loneragan JF (1967) Response of plants to phosphate concentration in solution culture: growth and phosphorus content. *Soil Sci* **103**, 225–233.
51 Hoops S, Sahle S, Gauges R, Lee C, Pahle J, Simus N, Singhal M, Xu L, Mendes P & Kummer U (2006) COPASI – a COmplex PAthway SImulator. *Bioinformatics* **22**, 3067–3074.
52 Schomburg I, Chang A & Schomburg D (2002) BRENDA, enzyme data and metabolic information. *Nucleic Acids Res* **30**, 47–49.
53 Wittig U, Golebiewski M, Kania R, Krebs O, Mir S, Weidemann A, Anstein S, Saric J & Rojas I (2006) SABIO-RK: integration and curation of reaction kinetics data. In *Proceedings of the 3rd International workshop on Data Integration in the Life Sciences 2006 (DILS'06). Hinxton, UK. Lecture Notes in Bioinformatics*, pp. 94–103.
54 Even S, Lindley ND, Loubière P & Cocaign-Bousquet M (2002) Dynamic response of catabolic pathways to autoacidification in *Lactococcus lactis*: transcript profiling and stability in relation to metabolic and energetic constraints. *Mol Microbiol* **45**, 1143–1152.
55 Even S, Lindley ND & Cocaign-Bousquet M (2001) Molecular physiology of sugar catabolism in *Lactococcus lactis* IL1403. *J Bacteriol* **183**, 3817–3824.
56 Rimpiläinen MA, Mettänen TT, Niskasaari K & Forsén RI (1988) The F1-ATPase from *Streptococcus cremoris*: isolation, purification and partial characterization. *Int J Biochem* **20**, 1117–1124.
57 Cvitkovitch DG, Boyd DA, Thevenot T & Hamilton IR (1995) Glucose transport by a mutant of *Streptococcus mutans* unable to accumulate sugars via the phosphoenolpyruvate phosphotransferase system. *J Bacteriol* **177**, 2251–2258.
58 Simon WA & Hofer HW (1981) Phosphofructokinases from Lactobacteriaceae. II. Purification and properties of phosphofructokinase from *Streptococcus thermophilus*. *Biochim Biophys Acta* **661**, 158–163.
59 Crow VL & Pritchard GG (1982) Pyruvate kinase from *Streptococcus lactis*. *Methods Enzymol* **90** (Pt E), 165–170.
60 Crow VL & Wittenberger CL (1979) Separation and properties of NAD^+- and $NADP^+$-dependent glyceraldehyde-3-phosphate dehydrogenases from *Streptococcus mutans*. *J Biol Chem* **254**, 1134–1142.
61 Iddar A, Serrano A & Soukri A (2002) A phosphate-stimulated $NAD(P)^+$-dependent glyceraldehyde-3-phosphate dehydrogenase in *Bacillus cereus*. *FEMS Microbiol Lett* **211**, 29–35.
62 Brown CK, Kuhlman PL, Mattingly S, Slates K, Calie PJ & Farrar WW (1998) A model of the quaternary structure of enolases, based on structural and evolutionary analysis of the octameric enolase from *Bacillus subtilis*. *J Protein Chem* **17**, 855–866.
63 Takahashi S, Abbe K & Yamada T (1982) Purification of pyruvate formate-lyase from *Streptococcus mutans* and its regulatory properties. *J Bacteriol* **149**, 1034–1040.
64 Sutton SV & Marquis RE (1987) Membrane-associated and solubilized ATPases of *Streptococcus mutans* and *Streptococcus sanguis*. *J Dent Res* **66**, 1095–1098.
65 Sommer P, Klein JP, Schöller M & Frank RM (1985) Lactate dehydrogenase from *Streptococcus mutans*: purification, characterization, and crossed antigenicity with lactate dehydrogenases from *Lactobacillus casei*, *Actinomyces viscosus*, and *Streptococcus sanguis*. *Infect Immun* **47**, 489–495.
66 Liebermeister W & Klipp E (2006) Bringing metabolic networks to life: convenience rate law and thermodynamic constraints. *Theor Biol Med Model* **3**, 41.
67 Liebermeister W & Klipp E (2006) Bringing metabolic networks to life: integration of kinetic, metabolic, and proteomic data. *Theor Biol Med Model* **3**, 42.
68 Jonsson M, Saleihan Z, Nes IF & Holo H (2009) Construction and characterization of three lactate dehydrogenase-negative *Enterococcus faecalis* V583 mutants. *Appl Environ Microbiol* **75**, 4901–4903.
69 Köller T, Nelson D, Nakata M, Kreutzer M, Fischetti VA, Glocker MO, Podbielski A & Kreikemeyer B (2008) PlyC, a novel bacteriophage lysin for compartment-dependent proteomics of group A streptococci. *Proteomics* **8**, 140–148.
70 Nelson D, Schuch R, Chahales P, Zhu S & Fischetti VA (2006) PlyC: a multimeric bacteriophage lysin. *Proc Natl Acad Sci USA* **103**, 10765–10770.
71 Reizer J, Deutscher J, Sutrina S, Thompson J & Saier MH Jr (1985) Sugar accumulation in gram-positive

bacteria: exclusion and expulsion mechanisms. *Trends Biochem Sci* **10**, 32–34.
72 Kulaev I & Kulakovskaya T (2000) Polyphosphate and phosphate pump. *Annu Rev Microbiol* **54**, 709–734.

Supporting information

The following supplementary material is available:
Fig. S1. Metabolic profiles of a 25 mM glucose-pulse experiments in *L. lactis*.
Data S1. *L. lactis* glycolysis model.
Table S1. Velocity constants (in mM/s or mmol/s).
Table S2. Reversible processes: K_{eq}.
Table S3. Michaelis constants K_m (mM).
Table S4. Allosteric regulation binding constants: activation K_a (mM) and inhibition K_i (mM).
Table S5. Hill coefficients.
Table S6. Initial concentrations (mM) for 10 and 50 mM extracellular phosphate as well as for ^{13}C- and ^{31}P-NMR data of Neves *et al*. [17].
Data S2. Rate laws of the *L. lactis* glycolysis model.
Data S3. Differential equations and moiety conservation of the *L. lactis* model.
Data S4. *S. pyogenes* glycolysis model.
Data S5. Rate laws of the *S. pyogenes* model.
Data S6. Differential equations and moiety conservation of the *S. pyogenes* model.
Table S7. Velocity constants (in mM/s or mmol/s).
Table S8. Reversible processes: K_{eq}.
Table S9. Michaelis constants: K_m (mM).
Table S10. Allosteric regulation binding constants (mM).
Table S11. Hill coefficients.
Table S12. Initial concentrations (mM) for 0, 10 and 50 mM extracellular phosphate.

This supplementary material can be found in the online version of this article.

Please note: As a service to our authors and readers, this journal provides supporting information supplied by the authors. Such materials are peer-reviewed and may be re-organized for online delivery, but are not copy-edited or typeset. Technical support issues arising from supporting information (other than missing files) should be addressed to the authors.